G PROTEIN-COUPLED RECEPTORS

NEW OPPORTUNITIES FOR COMMERCIAL DEVELOPMENT

Editor:

Nancy Mulford

Managing Editor:

Lynn M. Savage

BIOMEDICAL LIBRARY SERIES

International Business Communications, Inc.

Chapter 6.3

Molecular Mechanism of Signal Transduction by Rhodopsin

Thomas P. Sakmar, M.D., Howard Hughes Medical Institute, Rockefeller University

Our laboratory is interested in the molecular mechanism of G protein-mediated signal transduction. We have chosen to study the vertebrate visual system as a model of G protein-mediated signaling. In particular, we study the visual photoreceptor molecule, rhodopsin, and the visual G protein, transducin. We have initially focused on the receptor activation process and also on receptor-G protein interaction. We have also recently begun to study G protein-effector enzyme interactions.

The work I will discuss in this chapter will refer exclusively to rhodopsin and to the structural information concerning this receptor that can be obtained by a variety of biophysical methods. Rhodopsin is the photoreceptor molecule of the retinal rod cell, the cell responsible for dim light vision. These cells are noteworthy because they have a highly specialized rod outer segment (ROS) separated from the inner segment by a narrow cilium. The ROS is stacked with disk membranes. The disk membranes contain a high proportion of rhodopsin, an integral membrane protein. Isomerization of the rhodopsin chromophore, which is the aldehyde of vitamin A linked to the opsin apoprotein via a protonated Schiff base linkage, causes a cascade of biochemical events leading to a graded hyperpolarization of the plasma membrane of the rod cell.

Figure 1 shows a schematic primary and secondary structural model of bovine rhodopsin. In the orientation presented, the amino terminus or extracellular surface is towards the bottom and the carboxyl terminus or cytoplasmic surface is towards the top of the figure. The topological orientation of the receptor is inverted, compared to other G protein-coupled receptors presented in this proceedings. Bovine rhodopsin was sequenced at the amino acid level by classical methods[1,2] and was also the first G protein-coupled receptor to be cloned.[3] At this point there are probably about 100 visual pigments that have been characterized, including the three cone pigments responsible for human trichromatic color vision.[4]

The chromophore of nearly all visual pigments, including rhodopsin, is 11-*cis* -retinal. The chromophore of a visual pigment is analogous to a ligand of a typical G protein-coupled receptor.[5] However, it is actually a co-factor since it is covalently bonded to the opsin apoprotein via a protonated Schiff-based linkage (a C=N linkage) to a specific lysine residue on transmembrane (TM) helix 7 of the opsin (Fig. 1). The cis to trans photochemical isomerization of retinal (Fig. 2) is the only light-dependent event in

vision. The remaining molecular processes of vision involve thermal and biochemical events.

In our laboratory, we use a well-established system for structure-function studies of visual pigments. The heterologous expression and purification of visual pigments was originally pioneered by the laboratory of H. Gobind Khorana at the Massachusetts Institute of Technology.[6] This procedure involves the expression of a synthetic gene for the bovine opsin in COS cells, or in other cultured cell lines. The cells can then be incubated in the dark with 11-*cis* -retinal to form the pigment. The cells, which now contain regenerated visual pigment in their plasma membranes, can be solubilized in detergent if required. After regeneration, many visual pigment molecules are fairly stable in solution in a variety of detergents. We generally employ dodecylmaltoside, a non-denaturing, non-ionic detergent, but other detergents can be used as well. A detergent extract of transfected cells expressing recombinant rhodopsin can be incubated with an immunoaffinity resin that consists of a monoclonal antibody that recognizes the carboxyl terminal eight amino acids of the molecule (Fig. 1). Under certain conditions, rhodopsin binds specifically to the resin, and washing removes any non-specifically bound material. The purified recombinant pigment can then be eluded from the resin by competition with a peptide that corresponds to the monoclonal antibody epitope.

If this type of procedure is carried out, UV-visible spectroscopy can be performed on the recombinant pigment because it is recovered as a detergent solubilized sample. Figure 3 shows a UV-visible spectrum of recombinant rhodopsin purified from COS cells. The solid line shows the UV-visible spectrum of rhodopsin (Rho) in the dark. A 280 nm peak is characteristic of the opsin apoprotein constituent and the 500 nm peak results from the 11-*cis*-retinal chromophore. If the 500 nm peak is illuminated, isomerization takes place and the protonated Schiff base of the chromophore linkage becomes deprotonated, which shifts the absorption spectrum from 500 nm to 380 nm. The 380 nm spectral form of rhodopsin is known as metarhodopsin II (meta II or MII) and is the active form of the receptor which interacts with the heterotrimeric G protein of the rod cell, transducin.

A number of assays have been used to study the ability of rhodopsin, and of mutant rhodopsins, to activate transducin. One assay takes advantage of the observation of A. Gilman[7] that the GTP (guanosine triphosphate)-bound active form of α subunits of heterotrimeric G proteins have a much higher intrinsic tryptophan fluorescence than the GDP (guanosine diphosphate)-bound inactive form. We developed a time-resolved

assay, which is used to monitor transducin activation by recombinant pigment, as shown in Figure 4. In this example, relative fluorescence intensity as plotted as a function of time. The baseline fluorescence of a detergent-buffer solution containing transducin alone is first measured. Rhodopsin is then added under continuous illumination, which causes a slight increase in fluorescence because of the addition of protein. When GTPγS, a non-hydrolyzable analogue of GTP, is added, a dramatic fluorescence increase is recorded as a function of time. This is because the injection of GTPγS in the presence of rhodopsin causes loading of the transducin with the GTPγS, which causes an increase in the concentration of GTPγS-bound α subunit of transducin. From time courses such as that shown in Figure 4, specific kinetic information can be obtained about the light-dependent activation of transducin by rhodopsin.

We have used the expression system described above to perform structure-function studies on site-directed mutants of rhodopsin. We have made progress in understanding the mechanism of spectral tuning in visual pigments,[8] the specific nature of the chemical environment of the Schiff base chromophore linkage in rhodopsin,[9-12] and the mechanism of receptor-G protein interaction.[13-15] Using similar techniques, a number of other laboratories including H. G. Khorana's laboratory at M.I.T., D. Oprian's laboratory at Brandies University, J. Nathan's laboratory at Johns Hopkins University Medical School, and others have made significant contributions to addressing these problems as well.[16-18]

What higher order structural information is available about the molecules of the vertebrate visual transduction system? The work of Schertler et al.[19] provided a projection map of reconstituted rhodopsin in phospholipid bilayers, as shown in Figure 5. It should be pointed out that the individual TM helices were not assigned to particular densities in this map. However, with the information in Figure 5 as a starting point, Joyce Baldwin carried out an exhaustive survey of the primary structures and properties of 204 G protein-coupled receptors and was able to assign tentatively the helices to the projection map densities.[20] According to her assignments, the 7 putative TM helices are contiguous with TM helix 3 being in the center of the helical bundle. TM helices 4 through 7 are the most well defined in the density map. Using these TM helix assignments, the primary structure of rhodopsin, the location of the specific lysine residue that forms the Schiff base bound with 11-*cis*-retinal, and the crystal structure of 11-*cis*-retinal, it is possible to create molecular graphics models of rhodopsin and related G protein-coupled receptors. One such model was created by Dr. S. W. Lin in our

laboratory and is available on the World Wide Web G Protein-Coupled Receptor Data Base at http://swift.embl-heidelberg.de/7tm/. When viewing this model, the small size of the 11-*cis*-retinal is striking when compared with the size of the overall receptor, and the key question of how the signal of retinal isomerization is transmitted from the membrane-embedded core of the receptor to its cytoplasmic surface immediately comes to mind.

High resolution crystal structures of the active and inactive forms of the transducin α subunit and the transducin heterotrimer are now available as well.[21, 22]

With this type of structural information, we can address some of the questions about molecular mechanism of transducin activation by rhodopsin. The key question is how does rhodopsin catalyze a conformational change in transducin, which leads to a change in its nucleotide-binding specificity? We have used two experimental approaches in our laboratory to address this question. The first approach is to identify rhodopsin mutants that have stable photo-intermediates or photo-intermediates that are uncoupled from the normal receptor activation pathway.[12, 23] The second approach is to use biophysical and spectroscopic methods, mainly vibrational spectroscopy, to study recombinant pigments.[24, 25] Only the second of these two approaches will be discussed in this chapter.

Vibrational spectroscopy can be divided into two main categories (Fig. 6). The first is Raman spectroscopy and the second is infrared (IR) spectroscopy. These two forms of vibrational spectroscopy are complementary. Raman spectroscopy provides information directly about the vibrational modes of the chromophore; whereas, IR spectroscopy provides structural information about the protein. We have previously employed resonance Raman spectroscopy in collaboration with R. Mathies at the University of California at Berkeley to study several mutant pigments.[26]

We have more recently employed Fourier-transform IR spectroscopy (FTIR) on recombinant pigments as well in collaboration with F. Siebert at Albert-Ludwigs-Universität in Freiburg, Germany. FTIR spectroscopy is simply an absorption difference technique. It has a fast time scale and is most sensitive to the protein environment, and in particularly to the vibrational modes of carbonyl and amide groups. FTIR is a very powerful technique to study rhodopsin because the photo-chemical isomerization of the chromophore, which occurs very quickly (tens of femtoseconds), is independent of temperature. All of the conformation changes of the protein, which occur after photo-chemical isomerization, are thermal. Therefore, rhodopsin can be frozen at liquid nitrogen temperature and illuminated to cause the isomerization. The protein, however, is

locked into a particular conformation called bathorhodopsin, which is characterized by a red-shifted absorption spectrum. As the sample is gradually warmed, the protein will actually snap into various meta-stable distinct spectral conformations, including lumirhodopsin, metarhodopsin I (MI), and MII (Fig. 7). MII is the rhodopsin photoproduct which activates transducin. The wavelength of maximal absorption values (λ_{max} values) for the intermediates in the activation pathway of rhodopsin shown in Figure 7 indicate that changes are occurring in terms of the interaction between the chromophore, which is now in the all-*trans* conformation, and the opsin apoprotein. But exactly what are the chemical nature of the changes?

This type of information can be obtained by FTIR-difference spectroscopy. Since a difference technique is employed, spectral data are obtained from the initial state of the receptor, for example the dark state of rhodopsin, at liquid nitrogen temperature. Then, the sample is illuminated to from bathorhodopsin. Additional spectral data are collected and the two spectra are subtracted to form a bathorhodopsin/rhodopsin difference spectrum as shown in the top spectrum of Figure 8, which is from the work of F. Siebert.[27] In the convention used here, the abscissa displays wavenumbers in reciprocal cm and the ordinate represents the absorbance change. Any positive deflections or peaks from the baseline arise from the photoproduct and any negative deflections or peaks arise from the initial state. If the sample is warmed gradually, other stable photoproducts can be elicited and the same difference technique applied. Figure 8 shows a collection of FTIR-difference spectra for the main photoproducts of rhodopsin in the rod cell disk membrane. For example, the metarhodopsin II (MII) difference spectrum is the IR vibrational-difference spectrum between MII and rhodopsin.

These spectra contain a significant amount of information. For example, in the region of 1,000 to 1,300 wavenumbers are the C-C and the C-H stretching frequencies that correspond to the retinal chromophore. The region from 1,700 to 1,800 wavenumbers is of particular interest, especially in the MII/Rho difference spectrum. This is the region of carbonyl stretch frequencies of protonated carboxylic acid groups. Although there is a significant wealth of chemical information in this collection of spectra, it has been somewhat inaccessible because none of the bands shown in Figure 8 have been definitively assigned to a particular group in the protein.

One of our main goals in using this technique in combination with techniques of molecular biology was to try to assign some of these bands so we could provide sight-specific structural information about specific photo-products of rhodopsin. To do this,

we concentrated on carboxylic acid groups, whose carbonyl stretching frequencies occupy a defined region of the spectrum. We initially mutated two carboxylic acid groups embedded in the TM core of the receptor, Asp-83 and Glu-122, which are located on TM helices 2 and 3, respectively (Fig. 9). The Glu-113 residue was also of interest because it has been shown to be the counterion to the protonated Schiff base chromophore linkage.[9, 28, 29] When the protein is folded up, the positive charge of the Schiff base at Lys-296 is neutralized by a negative charge at position Glu-113.

The two residues Asp-83 and Glu-122 were replaced by site-directed mutagenesis to form three mutants: Asp-83 to Asn (D83N), Glu-122 to Gln (E122Q), and the double mutant D83N/E122Q. The mutants were expressed in COS cells and purified as described above. The UV-visible spectrum of each mutant is shown in Figure 10. Several hundred micrograms of each mutant pigment was prepared and purified in order to carry out FTIR spectroscopy.

Figure 11 shows that the COS-cell rhodopsin, and the ROS rhodopsin from bovine retina, have very similar MII-difference spectra.[24] Spectra were also obtained for the 3 mutant pigments, which are generally similar to that of rhodopsin in the spectral region of 1,000 to 1,650 wavenumbers as shown. Figure 12 shows the same data with the area that was expected to be most affected by the mutation, 1,650 to 1,800 wavenumbers, expanded. Mutation of Glu-122 to Gln (E122Q), does not affect the first difference band with a negative peak at 1,767 wavenumbers, but abolishes the second band with a negative peak at 1,734 wavenumbers. Mutation of Asp-83 to Asn (D83N) has the opposite effect on the spectrum, with the first difference band abolished. In the double mutant D83N/E122Q, both difference bands are abolished, but a positive peak is still noted at 1,712 wavenumbers. The observation that two independent difference bands sensitive to mutation exist in this part of the spectrum indicates that residues Asp-83 and Glu-122 are protonated both in rhodopsin and in the MII photoproduct, the active state of the receptor. From the position of these bands, we can also infer information about hydrogen bonding, which is related to the frequency of the stretching vibration. For example, the hydrogen-bonding strength of Asp-83 increases, and the hydrogen-bond strength of Glu-122 decreases upon MII formation. The carbonyl stretch of Glu-113, which is the Schiff base counterion, is assigned to the positive band at 1,712 wavenumbers. It is already known that Glu-113 is negatively charged and unprotonated in ground state rhodopsin, and becomes protonated in the active state MII.[30]

With the vibrational frequency assignments as summarized in Figure 13, specific structural information, including protonation and hydrogen bonding in the active state and the ground state of rhodopsin, have become available for the first time.[24,25,30,31]

I would like to briefly focus on one other important amino acid residue in bovine rhodopsin, Glu-134. Figure 9 shows the location of Glu-134 on the cytoplasmic end of TM helix 3 of rhodopsin. The Glu or Asp/Arg charged pair at the cytoplasmic surface of TM helix 3 is highly conserved among the superfamily of G protein-coupled receptors. It has been known for some time that mutation of Glu-134 affects the ability of the active receptor to couple to transducin in two ways. First, D. Oprian's group showed that mutation of Glu-134 to Gln caused constitutive activity of the mutant opsin, meaning that the receptor was active even in the absence of a ligand chromophore.[32] Second, when we studied mutations at this position, we found the interesting phenotype shown in Figure 14, where three fluorescence activation assay traces are superimposed. Mutant pigment E134Q, under certain conditions, actually activates transducin more efficiently than wild-type rhodopsin. From detailed kinetic analysis of this mutant, we concluded that Glu-134 became protonated upon formation of the active state of rhodopsin.[33]

To show the protonation of Glu-134 directly, we turned to an old observation of G. Wald of Harvard University from the 1950s. When rhodopsin is photo-converted from the ground state to the active MII state, there is a net uptake of protons by the receptor. To show that this proton uptake might involve protonation of Glu-134, we collaborated with K. P. Hofmann, who is now at Humboldt University of Berlin.

We developed a method where we could simultaneously monitor the kinetics of formation of MII and the protonation of the MII species spectroscopically by using a pH-sensitive dye to monitor the pH change that accompanied the spectral change.

We studied two mutants: the E134Q mutant and the E134D mutant. The kinetics of the formation of the spectral MII-like form of each mutant was unaffected. Figure 15 shows the salient result of the analysis of the pH change after a flash of light for rhodopsin and the two mutants. When illuminated at time equals zero, rhodopsin takes up protons very rapidly and the pH comes to a new steady-state value. The mutant E134D also takes up protons with the same amplitude. However, the kinetics of the uptake are slowed down slightly, which might be expected from the fact that the Asp residue in the mutant has a slightly lower pKa value than Glu. The E134Q mutant is completely unable to take up protons, although it can form a MII species that can activate transducin normally or even hyperactively. This result is a striking biophysical

confirmation of the hypothesis that Glu-134 becomes protonated upon the formation of the active state of rhodopsin.[34]

In using the types of approaches described above, we feel that we are beginning to get some understanding of the structural differences between the ground state and the active state of rhodopsin. We are confident that these results will apply to many other G protein-coupled receptors as well, especially in cases where the residues under investigation are highly conserved.

In summary, we can look at a tentative molecular graphics model of rhodopsin (Fig. 16), which shows the results outlined in this chapter. In this orientation, the Glu-113 counterion is in close proximity to the Schiff base, which is positively charged. This carboxylate group becomes protonated by a net proton transfer from the Schiff base to Glu-113 upon photo-activation. Glu-122 and Asp-83 are protonated both in rhodopsin and in its active state. The hydrogen-bond strength of Asp-83 becomes stronger, and the hydrogen-bond strength of Glu-122 becomes weaker with receptor activation. Glu-134, which is on the cytoplasmic surface of TM helix 3, is most likely unprotonated in the ground state, and becomes protonated in the active state.

Acknowledgements

I would like to acknowledge the people in my laboratory who work on the vertebrate visual system: T. Zvyaga, C. Min, and S. Lin, and M. Han. L. Snyder studies the dopamine receptor, and A. Cypess and C. Unson study the glucagon receptor. A. You and S. Gravina study chemo-sensory taste transduction. I would also like to thank our collaborators, who have contributed to the work described in this chapter: K. P. Hofmann in Berlin, F. Siebert and K. Fahmy in Freiburg, and R. Mathies at Berkeley.

QUESTIONS AND ANSWERS

Question: Obviously, since most G-coupled receptors do not have a chromophore, you cannot use optical spectroscopic techniques to study them. What can you do?

Dr. Sakmar: Actually, there is an vibrational spectroscopy technique called attenuated total reflectance (ATR) spectroscopy, which involves FTIR technology. There is a two-chamber sample stage where the receptor can be in one chamber and a ligand can be diffused in from the other chamber through a dialysis membrane. Measurements are carried out in solution instead of on frozen dehydrated or partially hydrated samples. There is some hope that difference techniques could be applied to these systems. Also, if you have reconstituted membranes that have a high enough proportion of a G protein-coupled receptor of interest, there are other ways to freeze conformational states besides temperature. For example, pressure jumps, temperature jumps, and other things have been used in other systems. In addition, UV spectroscopy can be used generally to look at changes in the orientation of aromatic residues as receptors become activated.[35]

Comment: Schertler's structure is a projection structure, which is not a set of coordinates. There was a more recent paper, with a three-dimensional (3D) reconstruction of rhodopsin, that actually shows some of the things that many of the speakers in this meeting have been calling helices as being sort of blobs that might be unrecognizable as helices. This 3D structure should have more information than the projection structure. It looked like in all your pictures that the helices were actually quite parallel.

Dr. Sakmar: The models that I showed are not revised based on the latest Schertler projection maps.[36] They do not take into account the higher resolution frog rhodopsin structure that is now available. Although you might think that you gain information by seeing the dimension parallel to the membrane bilayer, it is actually at a very much lower resolution.

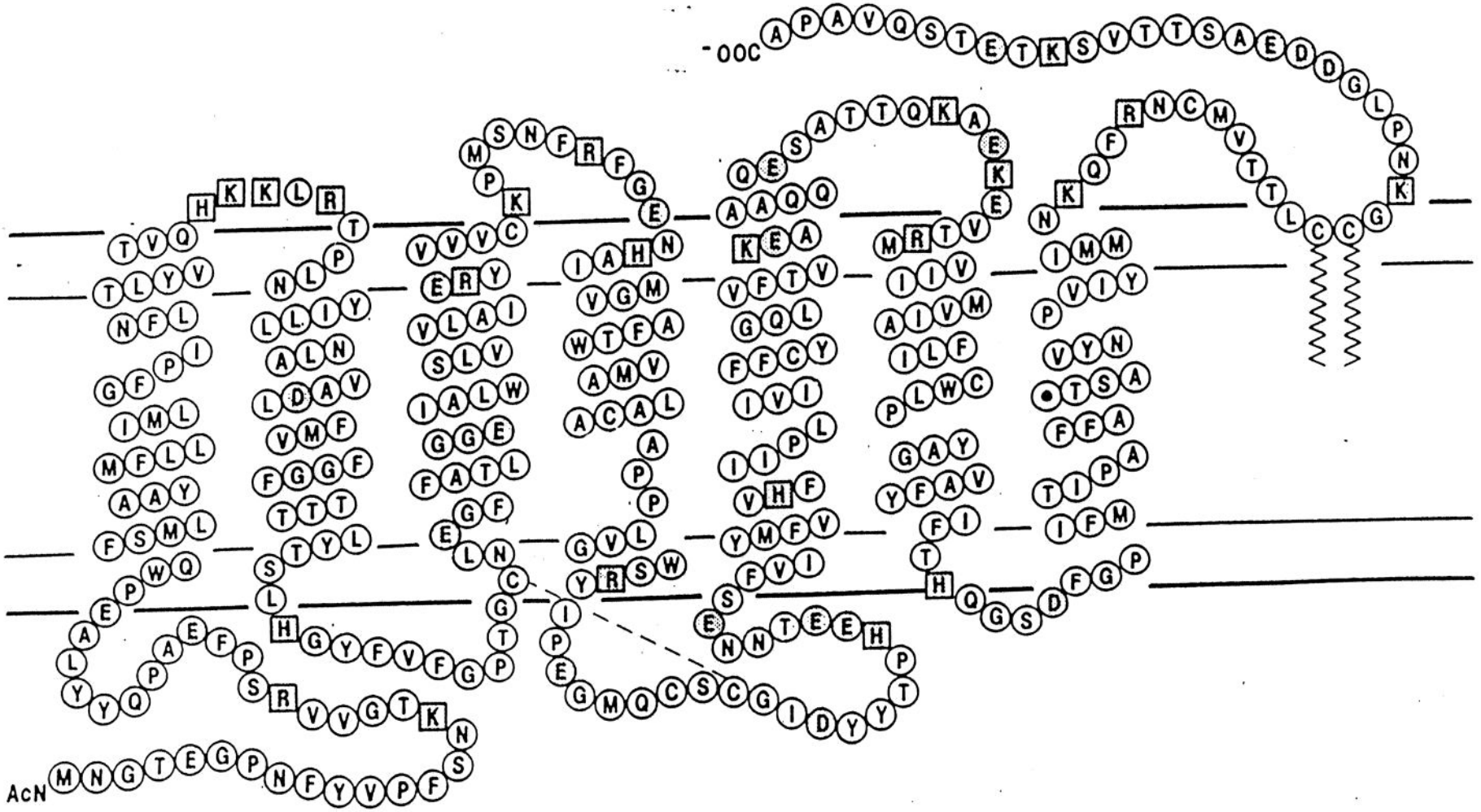

Figure 1. Schematic representation of the primary and secondary structure of bovine rhodopsin. The extracelluar surface and amino-terminal tail are towards the bottom and the cytoplasmic surface and carboxyl-terminal tail are towards the top of the figures. The seven putative TM helices are shown. An essential disulfide bond is indicated by a dotted line. (Compliments of W. Hubbell)

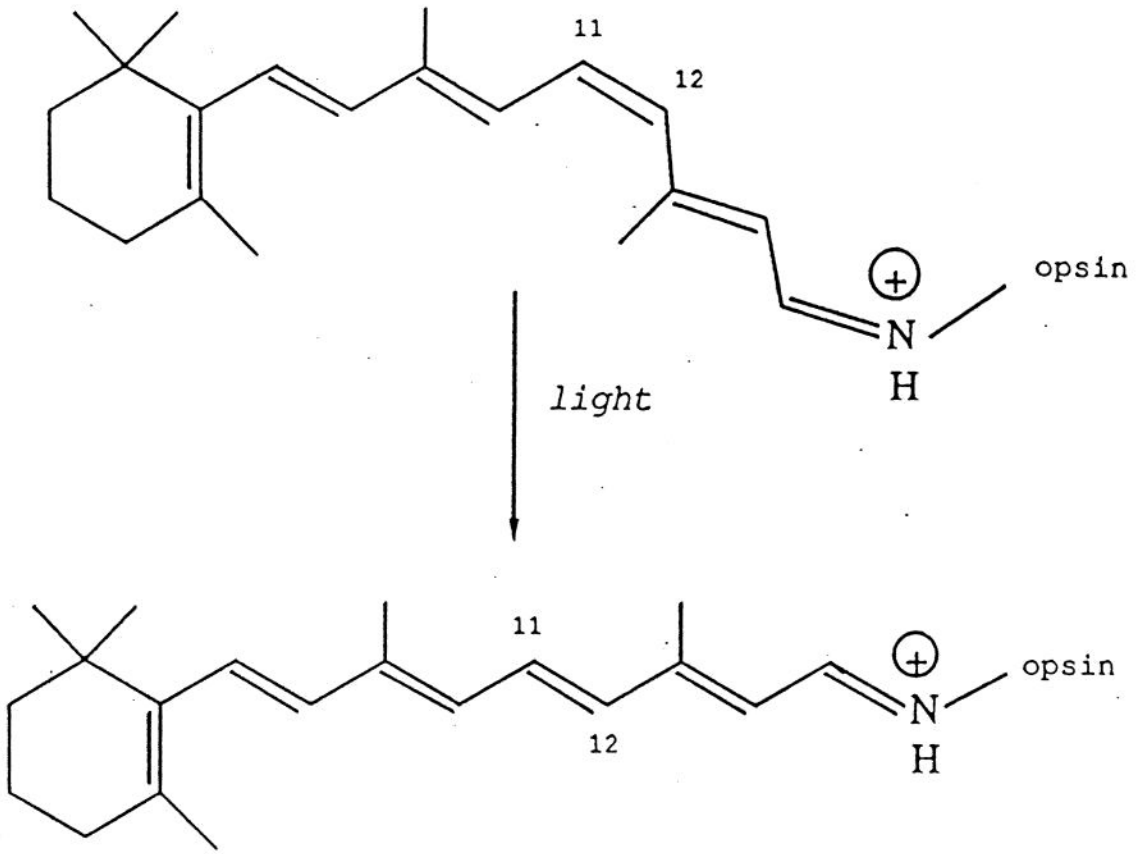

Figure 2. Photoisomerization of 11-*cis*-retinal to all-*trans*-retinal is the only light-dependent event in vision. The chromophore is covalently linked as a cofactor to a specific opsin lysine residue on TM helix 7 via a protonated Schiff base bond.

Adapted from Fig. 1 of Sakmar, T. P. (1994) in *Handbook of Receptors and Channels* (Vol. I: G Protein-coupled Receptors) (Peroutka, S. J., ed.) CRC Press, Boca Raton, v. I, pp. 257-276.

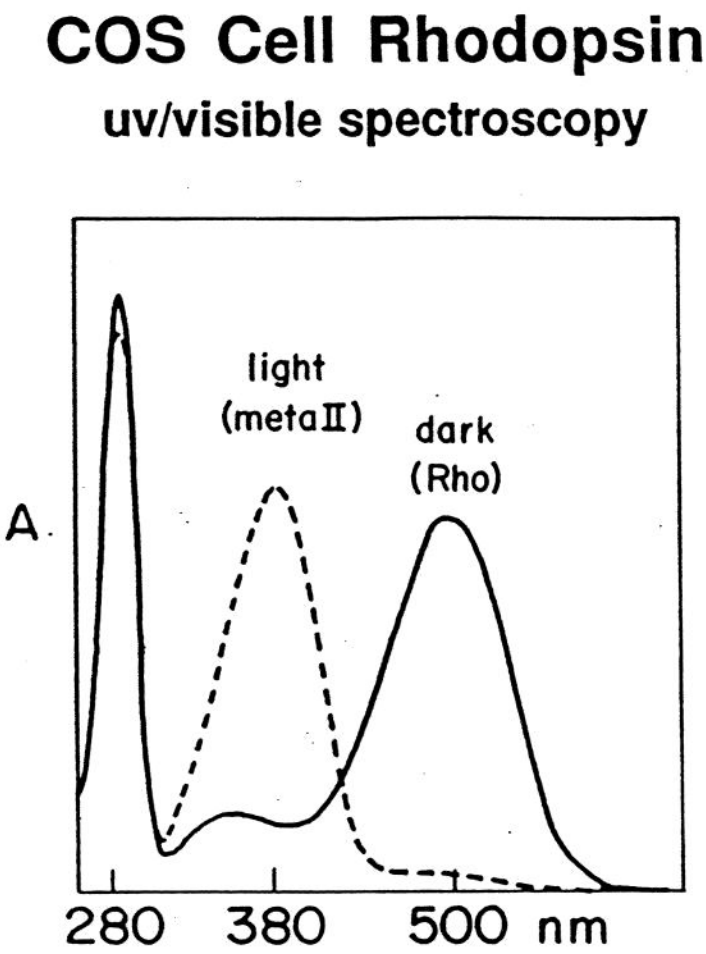

Figure 3. A UV-visible absorption spectrum of purified recombinant COS-cell rhodopsin shows a characteristic broad visible absorbance with a λ_{max} value of 500 nm. The 280-nm peak represents the protein component. After exposure to light, the pigment is converted to a peak with a λ_{max} value of 380 nm characteristic of MII. This is the active form of the receptor, which interacts with the ROS G protein, transducin.

Adapted from Fig. 2 of Sakmar, T. P. (1994) in *Handbook of Receptors and Channels* (Vol. I: G Protein-coupled Receptors) (Peroutka, S. J., ed.) CRC Press, Boca Raton, v. I, pp. 257-276.

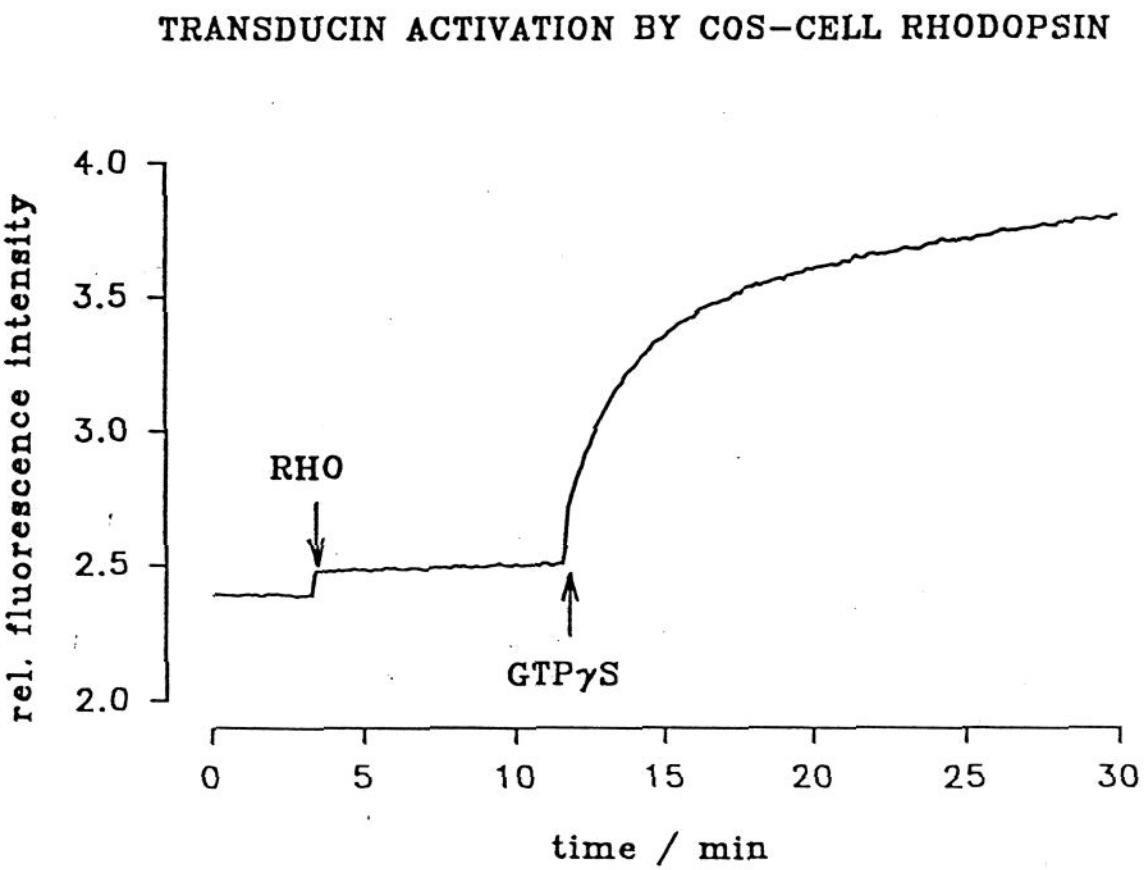

Figure 4. Fluorometric assay of rhodopsin-catalyzed GTPγS binding by transducin. A continuous time course of the relative intensity of fluorescence is shown. The assay mixture contains purified transducin. Rhodopsin (RHO) and GTPγS are added at the arrows as indicated.

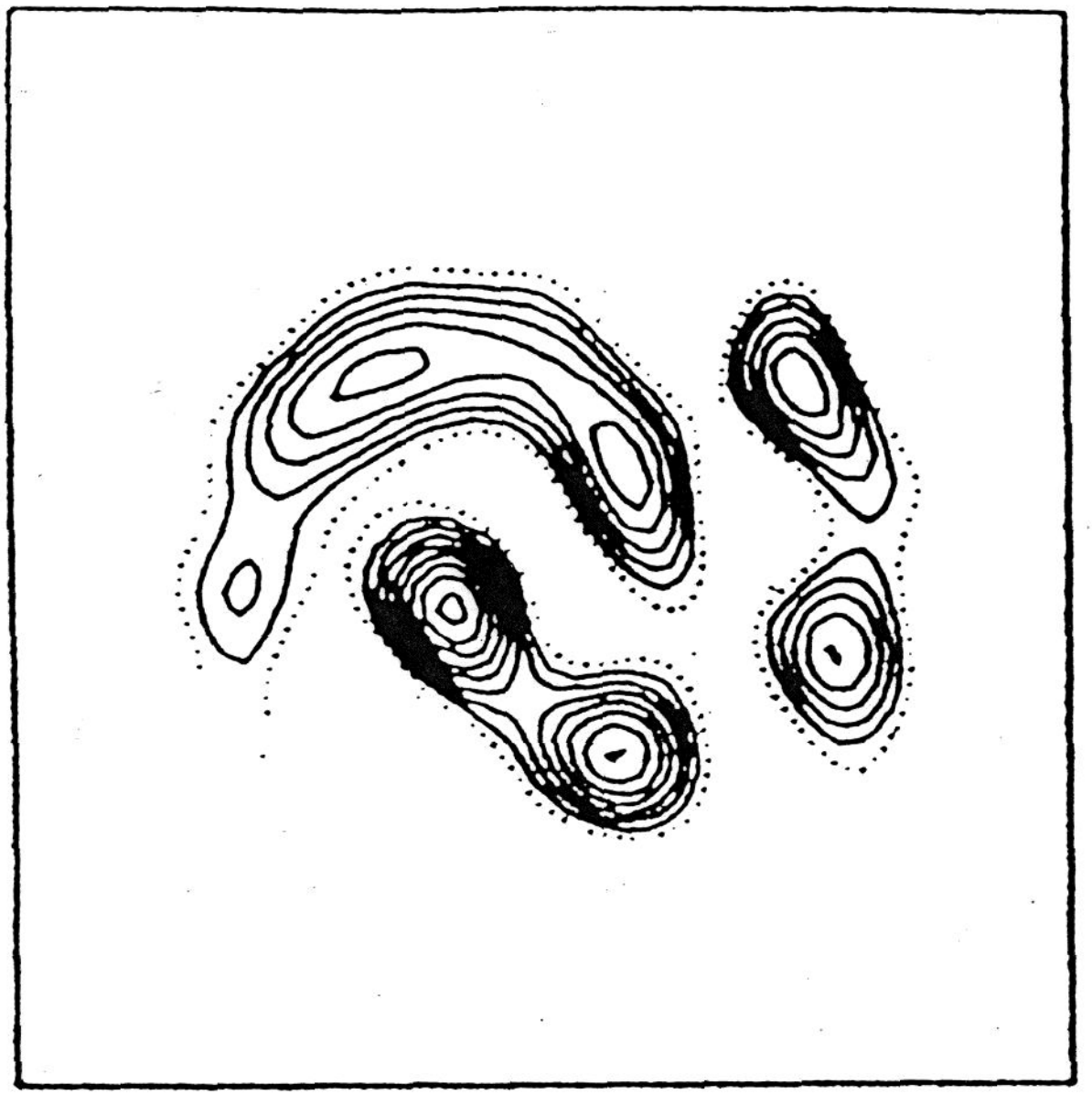

Figure 5. A projection density map of two-dimensional bovine rhodopsin crystals.[19] The densities have been tentatively assigned to the 7 TM helices of the receptor.[20]

Adapted from Schertler, C. F. X., Villa, C., and Henderson, R. (1993) *Nature* **362**: 770-772.

VIBRATIONAL SPECTROSCOPY

	Raman	Infrared
measurement:	difference in frequency between incident light & scattered light	ratio of transmitted to incident light as a function of wavelength
basis:	Raman effect	Beer-Lambert law
time scale:	10^{-15} s	10^{-15} s
most sensitive to:	chromophore (e.g. - C=C stretch)	protein (e.g. - C=O stretch)

Figure 6. A comparison of vibrational spectroscopic techniques applied to the study of visual pigments.

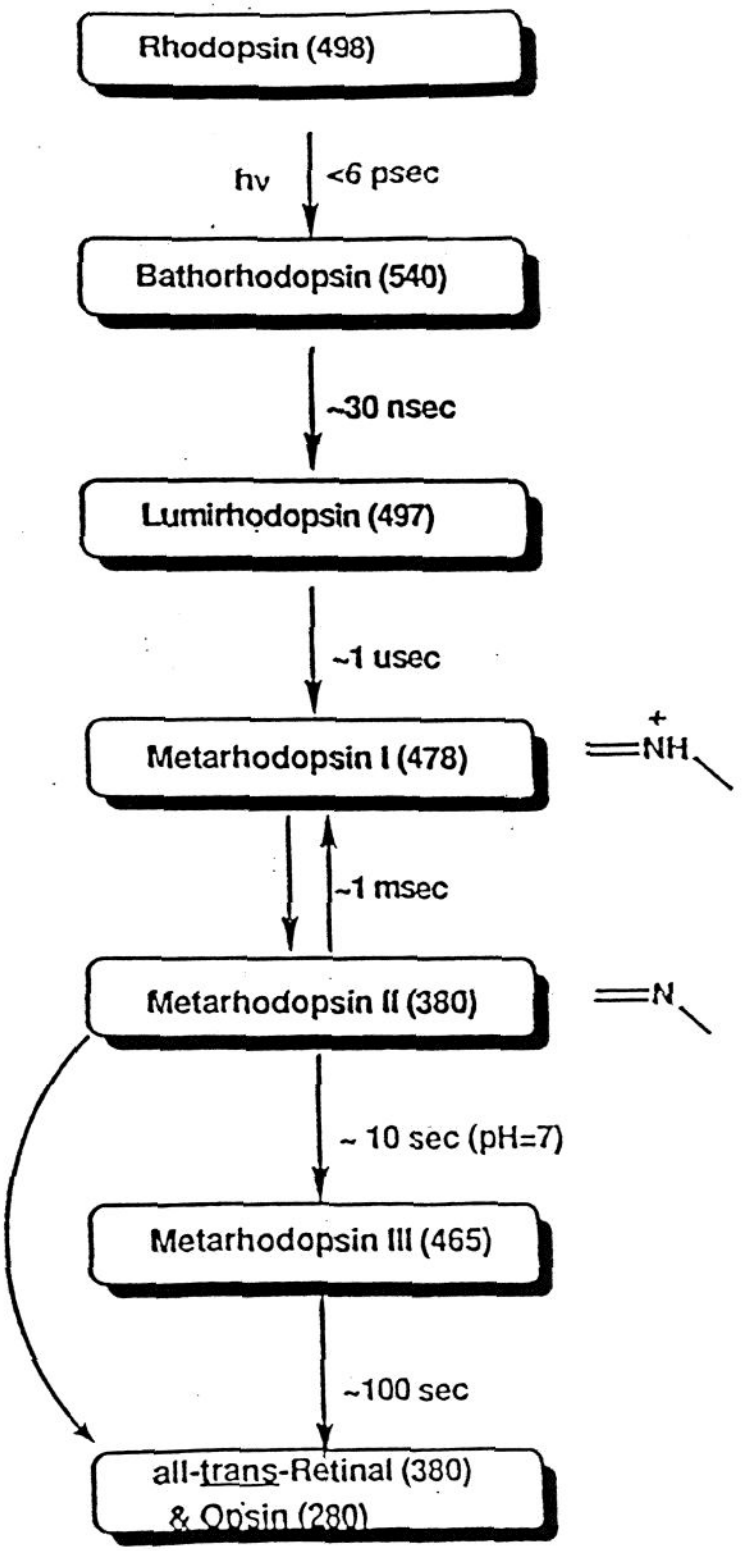

Figure 7. A schematic photoactivation pathway for bovine rhodopsin. The λ_{max} values for the intermediates are indicated in parentheses.

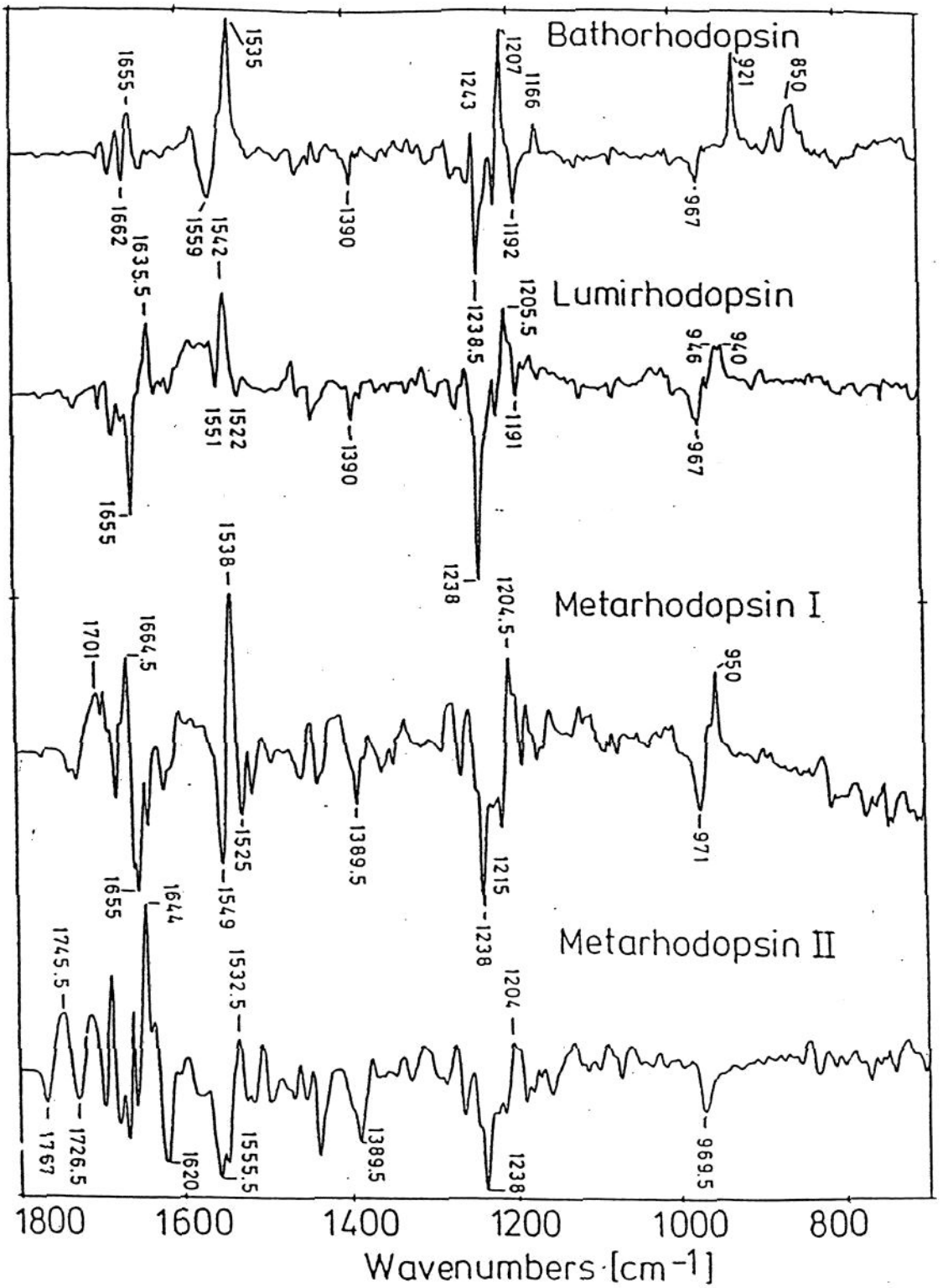

Figure 8. FTIR-difference spectra of bovine rhodopsin photoproducts.[27] Absorption bands of rhodopsin point downwards; those of the photoproducts point upwards.

Source: Siebert, F. *Methods Enzymol.* 189:123-136, 1990.

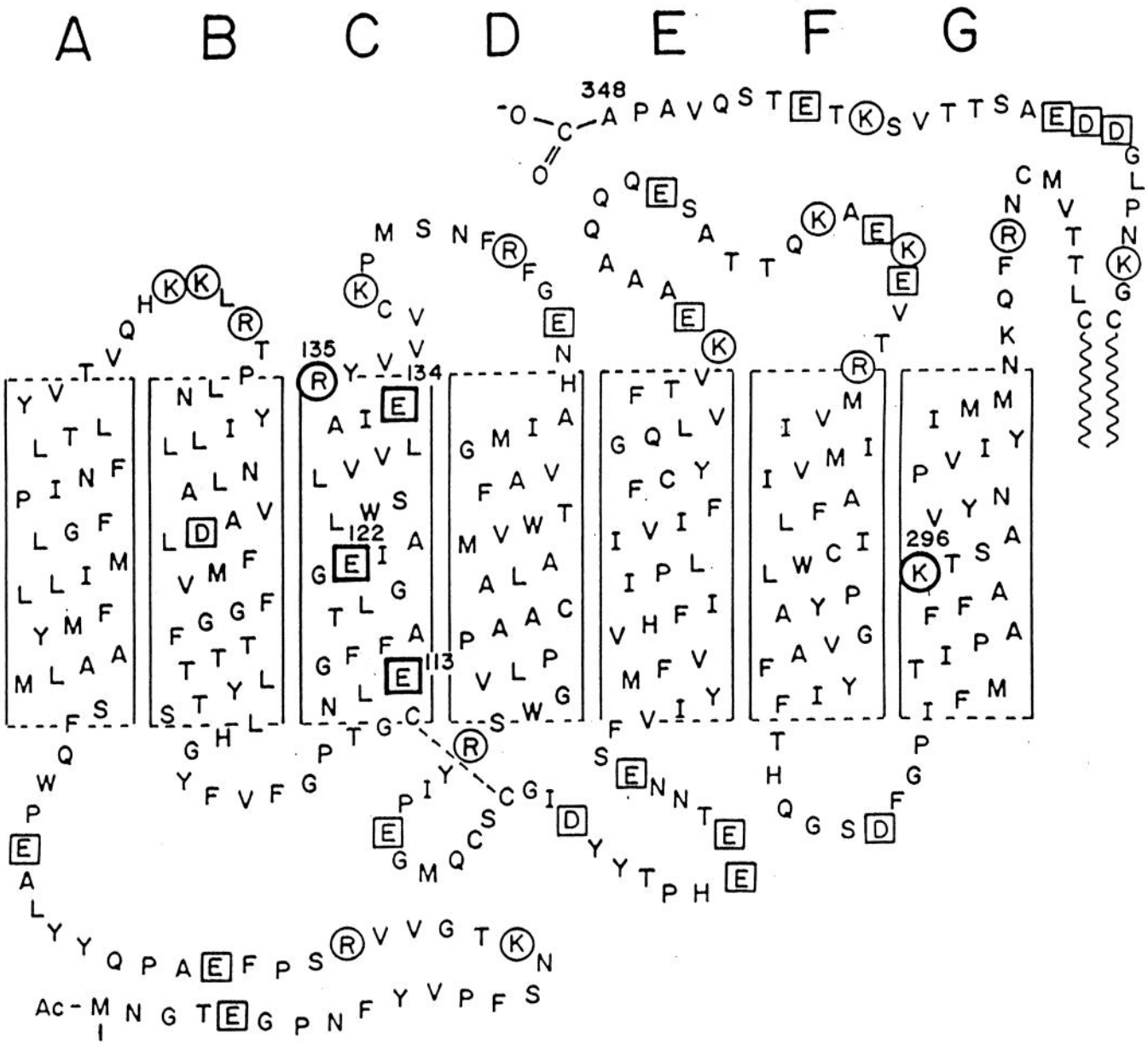

Figure 9. Schematic representation of the primary and secondary structure of bovine rhodopsin. Positively charged amino acid residues are circled and negatively charged amino acid residues are boxed. TM helix 3 contains four potentially charged residues.
Reprinted from Fig. 1 from Sakmar, T. P., Franke, R. R., and Khorana, H. G. (1989)*Proc. Natl. Acad. Sci. U.S.A.* **86**, 8309-8313, with permission from the National Academy of Sciences.

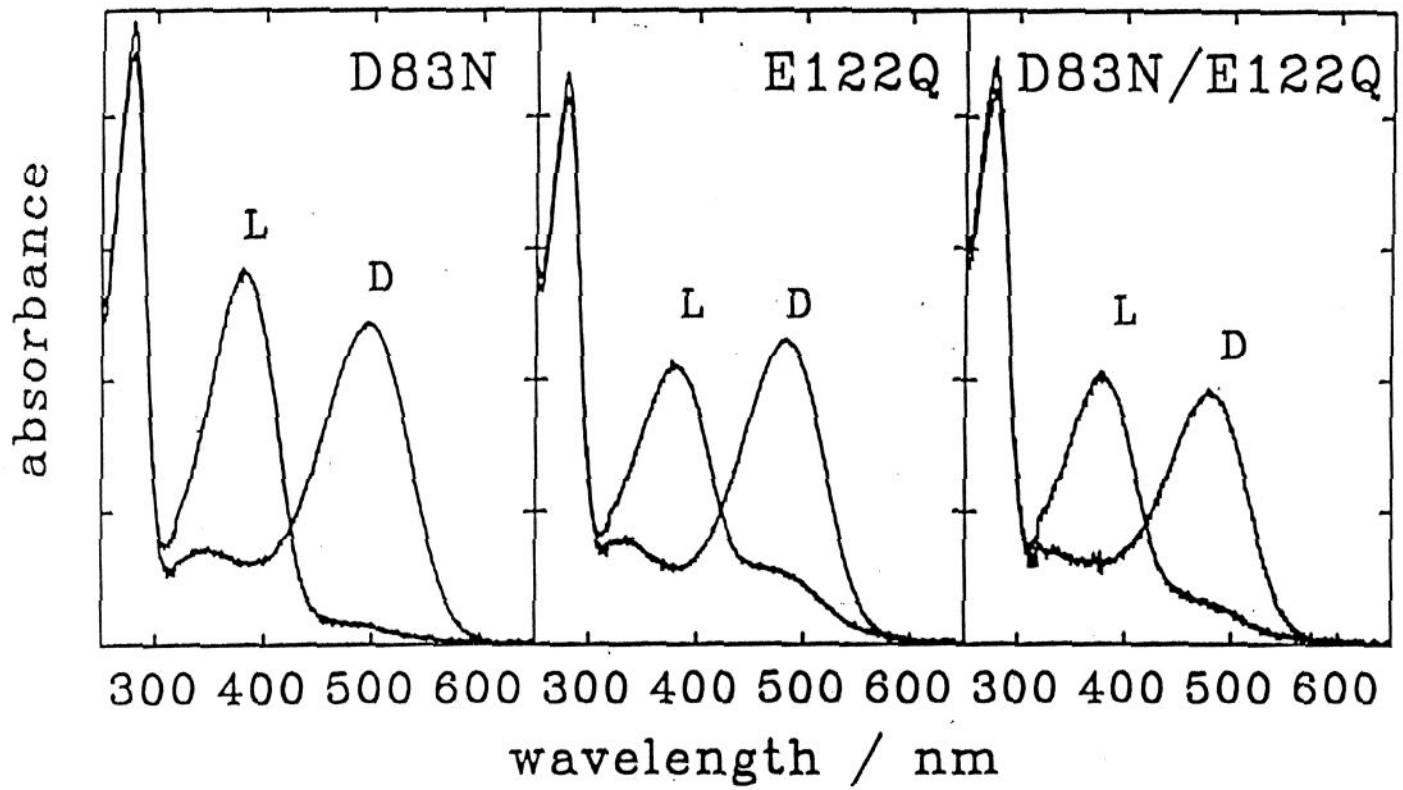

Figure 10. *UV-visible absorption spectra of mutant pigments subsequently studied by* FTIR spectroscopy. The dark spectrum (D) and spectrum after illumination (L) are shown for each mutant pigment.[24]

Reprinted from Fig. 1 from Fahmy, K., Jäger, F., Beck, M., Zvyaga, T. A., Sakmar, T. P., and Siebert, F. (1993)*Proc. Natl. Acad. Sci. U.S.A.* **90**: 10206-10210, with permission from the National Academy of Sciences.

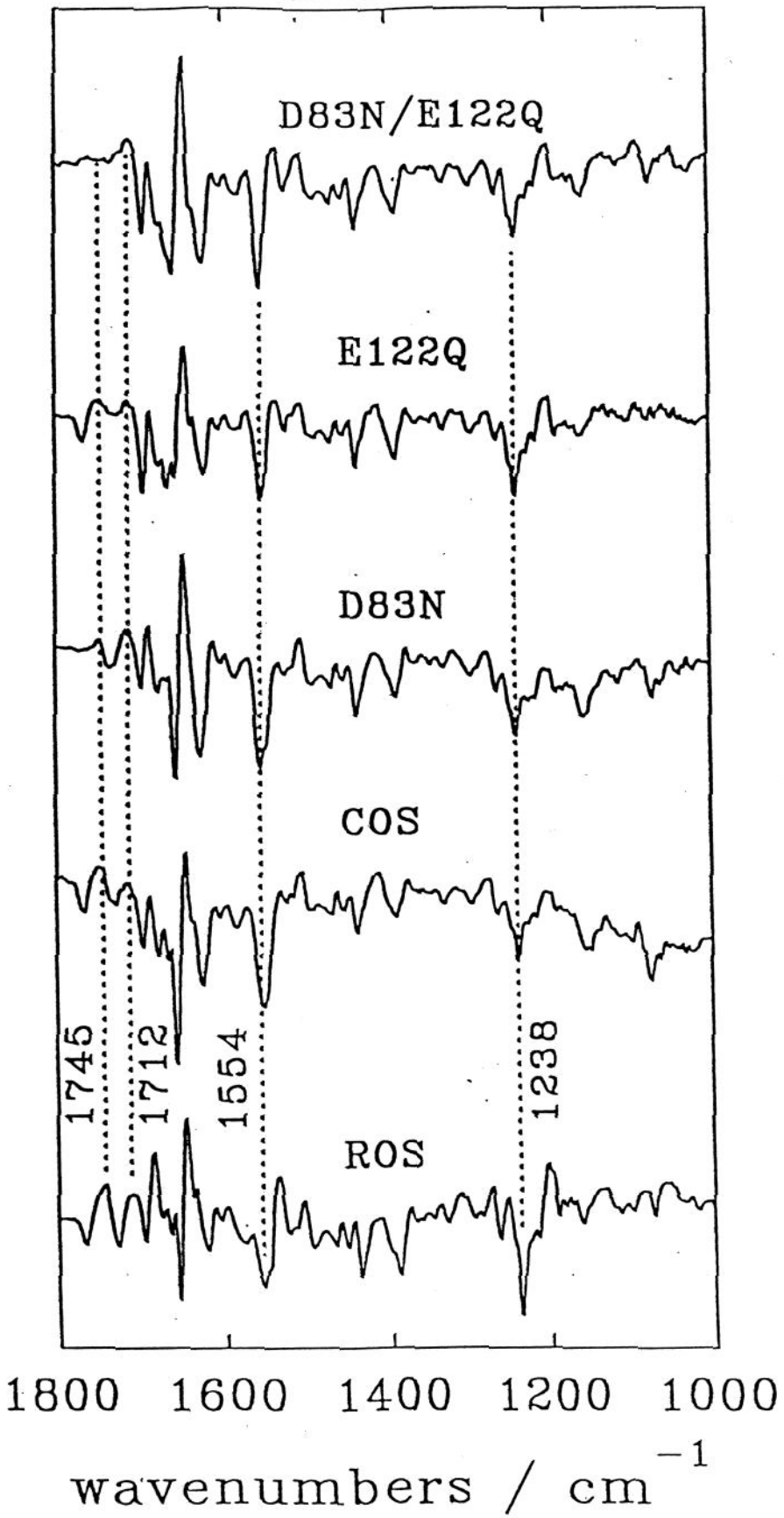

Figure 11. FTIR -difference spectra of rhodopsin in ROS membrane (ROS), recombinant COS-cell rhodopsin purified in the presence of detergent (COS), mutant D83N, mutant E122Q, and double mutant D83N/E122Q (from *bottom to top*).[24] *Reprinted from Fig. 3 from Fahmy, K., Jäger, F., Beck, M., Zvyaga, T. A., Sakmar, T. P., and* Siebert, F. (1993) *Proc. Natl. Acad. Sci. U.S.A.* 90: 10206-10210, with permission from the National Academy of Sciences.

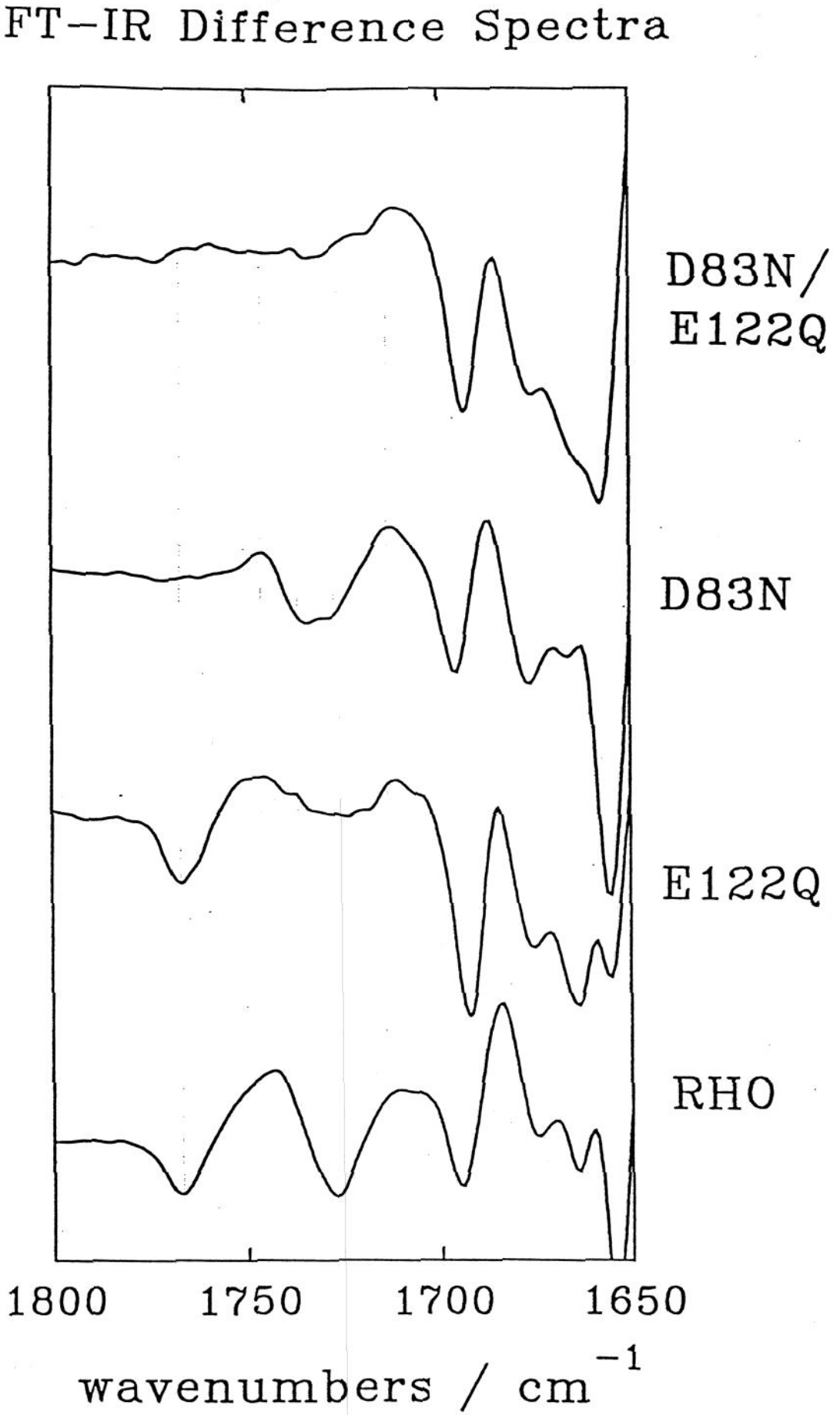

Figure 12. FTIR-difference spectra in the region of the carbonyl-stretching frequency of carboxylic acid groups. The data are taken from Figure 11.

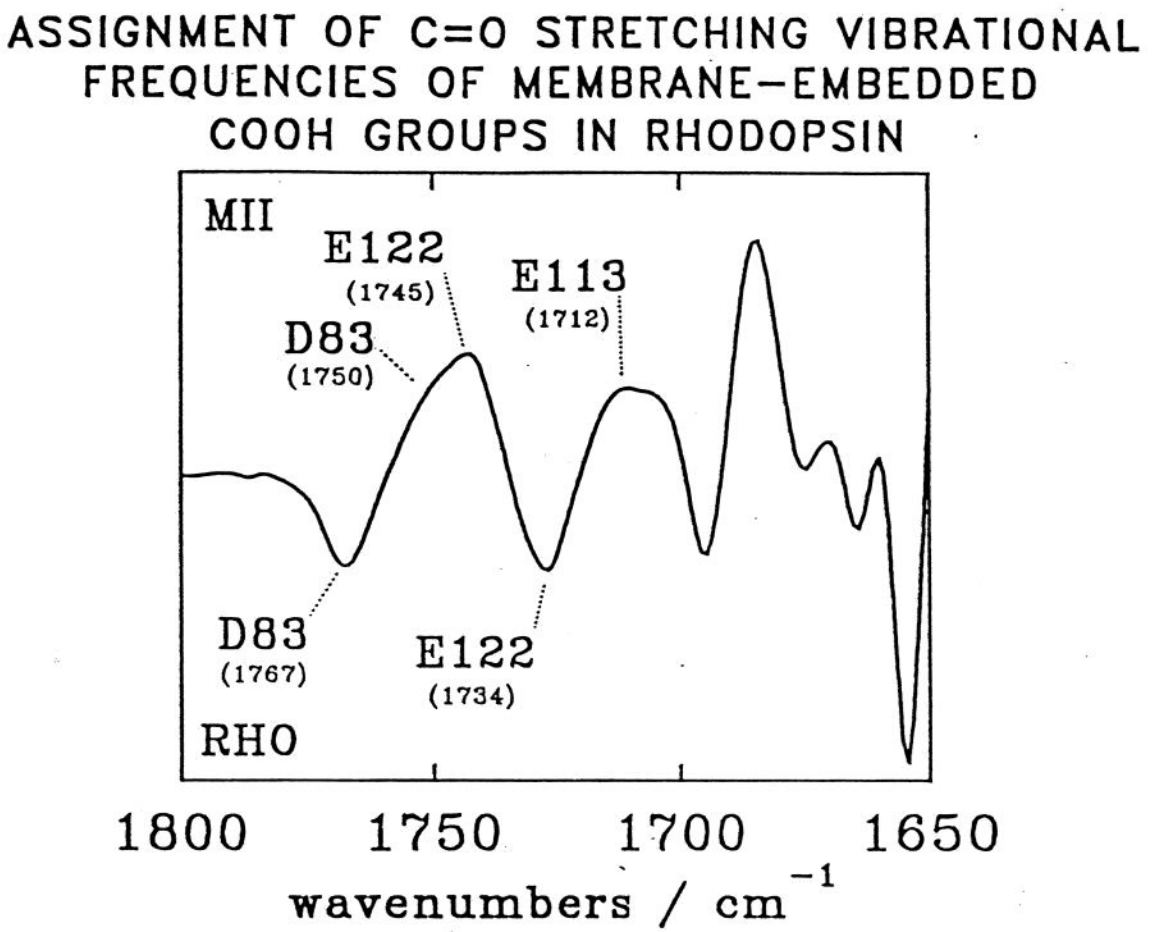

Figure 13. The assignment of carbonyl-stretching vibrational frequencies of membrane-embedded carboxylic acid groups in bovine rhodopsin.

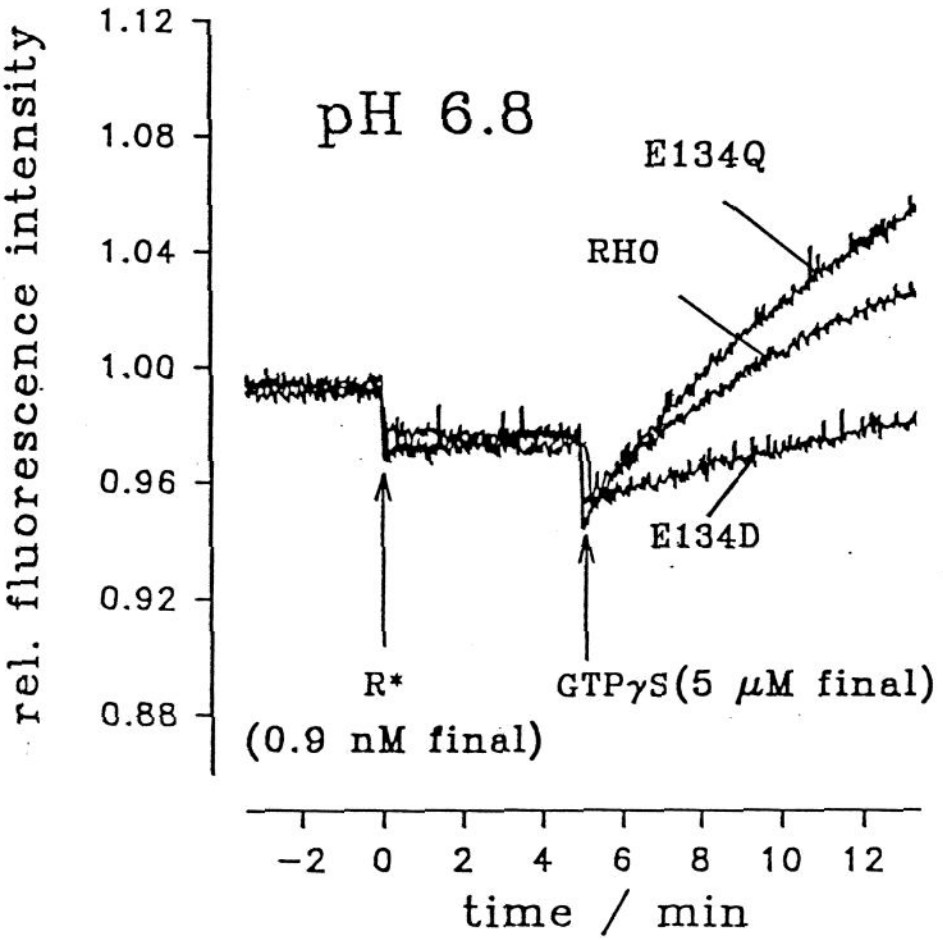

Figure 14. Time courses of transducin activation by recombinant pigments. The results of separate experiments for rhodopsin (RHO), mutant E134D, and mutant E134Q are superimposed.[33]

Adapted from Fig. 3 of Fahmy, K. and Sakmar, T. P. (1993) *Biochemistry* **32**: 7229-7236.

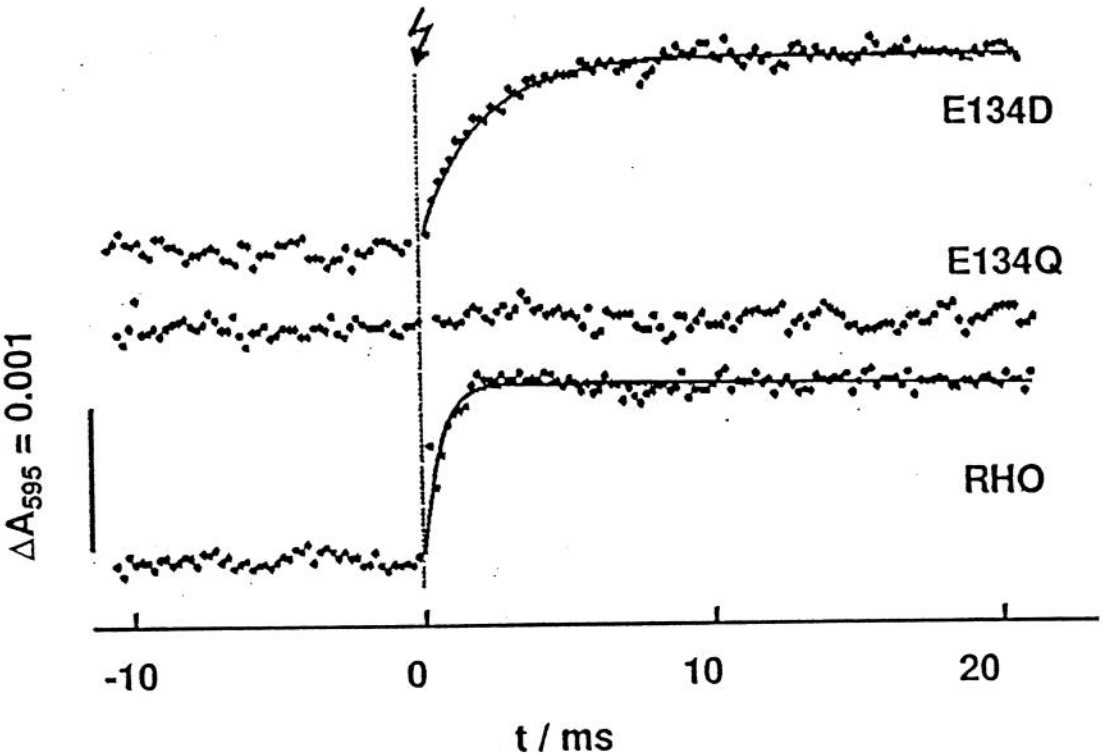

Figure 15. Kinetics of proton uptake in solutions of rhodopsin (RHO), E134Q, and E134D at pH 6. The arrow indicates a light flash[34].

Molecular Graphics Model of Bovine Rhodopsin

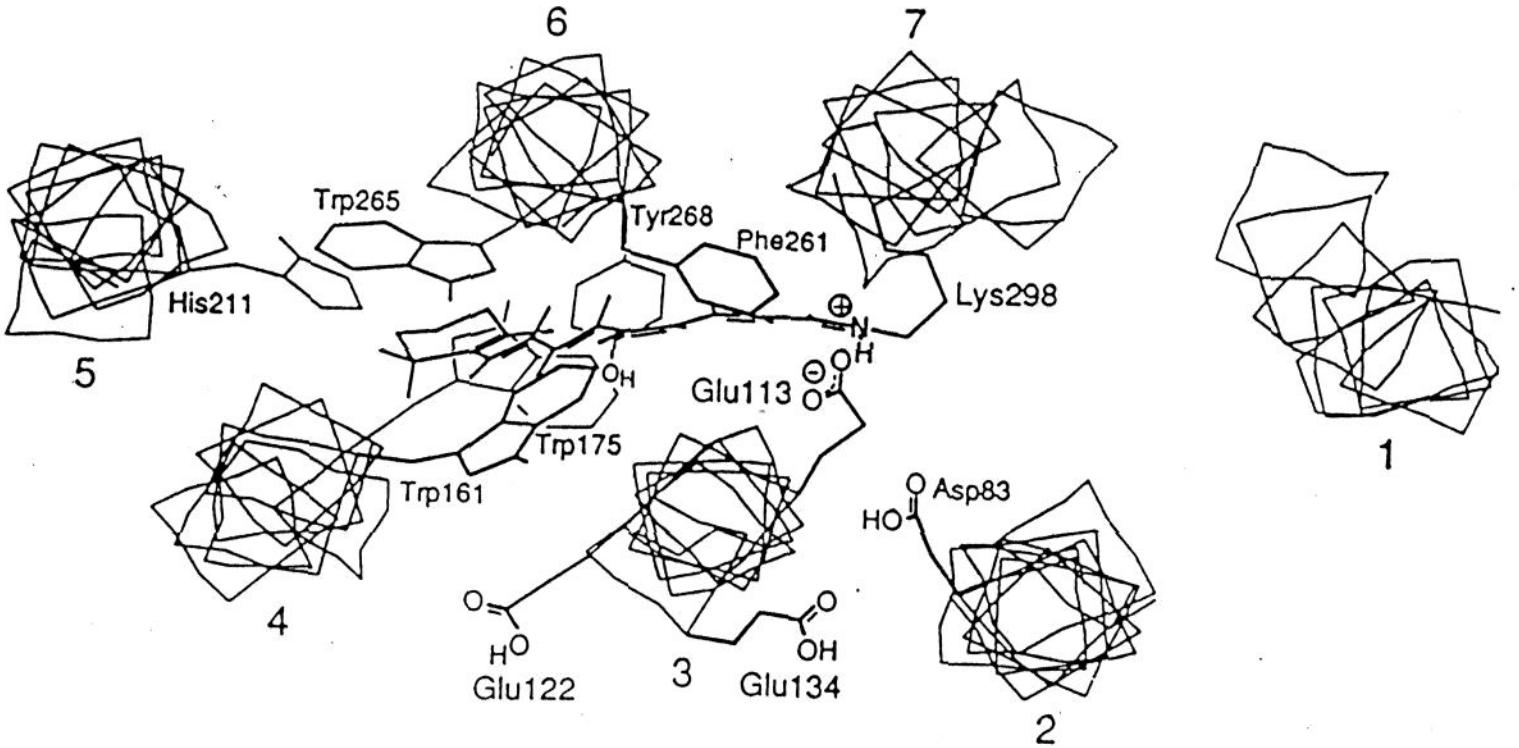

Figure 16. A molecular graphics model of the retinal-binding pocket of bovine rhodopsin. The pigment is viewed from above the plane of the membrane bilayer. *Selected amino acid side chains are displayed and numbered*[26].

Adapted from Fig. 6 of Lin, S. W., Sakmar, T. P., Franke, R. R., Khorana, H. G., and Mathies, R. A. (1992) *Biochemistry* **31**, 5105-5111.

REFERENCES

1. Hargrave, P. A., McDowell, J. H., Curtis, D. R., Wang, J. K., Jusczak, E., Fong, S. L., Mohanna Rao, J. K., and Argos, P. (1983) *Biophys. Struct. Mech.* **9**, 235-244.

2. Ovchinnikov, Y. A. (1982) *FEBS Lett.* **148**, 179-191.

3. Nathans, J. and Hogness, D. S. (1983) *Cell* **34**, 807-814.

4. Nathans, J., Thomas, D., and Hogness, D. S. (1986) *Science* **232**, 193-202.

5. Zhukovsky, E. A., Robinson, P. R., and Oprian, D. D. (1991) *Science* **251**, 558-560.

6. Oprian, D. D., Molday, R. S., Kaufman, R. J., and Khorana, H. G. (1987) *Proc. Natl. Acad. Sci. U.S.A. 84*, 8874-8878.

7. Higashijima, T., Ferguson, K. M., Smigel, M. D., and Gilman, A. G. (1987) *J. Biol. Chem. 262*, 757-761.

8. Chan, T., Lee, M., and Sakmar, T. P. (1992) *J. Biol. Chem.* **267**, 9478-9480.

9. Sakmar, T. P., Franke, R. R., and Khorana, H. G. (1989) *Proc. Natl. Acad. Sci. U.S.A.* **86**, 8309-8313.

10. Sakmar, T. P., Franke, R. R., and Khorana, H. G. (1991) *Proc. Natl. Acad. Sci. U.S.A.* **88**: 3079-3083.

11. Zvyaga, T. A., Min, K. C., Beck, M., and Sakmar, T. P. (1993) *J. Biol. Chem.* **268**: 4661-4667. Correction: *J. Biol. Chem.* **269**: 13056 (1994).

12. Zvyaga, T. A., Fahmy, K., and Sakmar, T. P. (1994) *Biochemistry* **33**: 9753-9761.

13. Franke, R. R., König, B., Sakmar, T. P., Khorana, H. G., and Hofmann, K. P. (1990) *Science* **250**, 123-125.

14. Franke, R. R., Sakmar, T. P., Graham, R. M., and Khorana, H. G. (1992) *J. Biol. Chem.* **267**, 14767-14774.

15. Ernst, O., Hofmann, K. P., and Sakmar, T. P. *J. Biol. Chem.* **270**: 10580-10586 (1995).

16. Khorana, H. G. (1992) *J. Biol. Chem.* **267**, 1-4.

17. Nathans, J. (1992) *Biochemistry* **31**, 4923-4930.

18. Sakmar, T. P. (1994) in *Handbook of Receptors and Channels* (Vol. I: G Protein-coupled Receptors) (Peroutka, S. J., ed.) CRC Press, Boca Raton, v. I, pp. 257-276.

19. Schertler, C. F. X., Villa, C., and Henderson, R. (1993) *Nature* **362**: 770-772.

20. Baldwin, J. M. (1993) *EMBO J.* **12:** 1693-1703.

21. Noel, J. P., Hamm, H. E., and Sigler, P. B. (1993) *Nature* **366**: 654-663

22. Lambright, D. G., Noel, J. P., Hamm, H. E., & Sigler, P. B. (1994) *Nature* **369**: 621-628

23. Fahmy, K., Siebert, F., and Sakmar, T. P. *Biochemistry* **33**: 13700-13705 (1994).

24. Fahmy, K., Jäger, F., Beck, M., Zvyaga, T. A., Sakmar, T. P., and Siebert, F. (1993) *Proc. Natl. Acad. Sci. U.S.A.* **90**: 10206-10210.

25. Rath, P., Lieveke, DeCaluwée, L. L. J., Bovee-Geurts, P. H. M., DeGrip, W. J., and Rothschild, K. J. (1993) *Biochemistry* **32:** 10277-10282

26. Lin, S. W., Sakmar, T. P., Franke, R. R., Khorana, H. G., and Mathies, R. A. (1992) *Biochemistry* **31**, 5105-5111.

27. Siebert, F. (1990) *Methods Enzymol.* **189**,123-136.

28. Zhukovsky, E. A. and Oprian, D. D. (1989) *Science* **246**: 928-930.

29. Nathans, J. (1990) *Biochemistry* **29**: 9746-9752.

30. Jäger, F., Fahmy, K., Sakmar, T. P., and Siebert, F. (1994) *Biochemistry* **33**: 10878-10882.

31. Fahmy, K., Siebert, F., and Sakmar, T. P. (1995) *Biophys. Chem.* **56**: 171-181.

32. Cohen, G. B., Oprian, D. D., and Robinson, P. R. (1992) *Biochemistry* **31**: 12592-12601.

33. Fahmy, K. and Sakmar, T. P. (1993) *Biochemistry* **32**: 7229-7236.

34. Arnis, S., Fahmy, K., Hofmann, K. P., and Sakmar, T. P. (1994) *J. Biol. Chem.* **269**: 23879-23881.

35. Lin, S. W. and Sakmar, T. P. (1996) *Biochemistry* (in press)

36. Schertler, C. F. X. and Hargrave, P. A. (1995) *Proc. Natl. Acad. Sci. U.S.A. 92*, 11578-11582.